Available online at www.sciencedirect.com
ScienceDirect
Journal of Sound and Vibration 320 (2009) 16–28
JOURNAL OF SOUND AND VIBRATION
www.elsevier.com/locate/jsvi

Nonlinear phase shift control of semi-active friction devices for optimal energy dissipation

Paulin Buaka Muanke, Philippe Micheau*, Patrice Masson

GAUS, Mechanical Engineering Department, Université de Sherbrooke, Sherbrooke, Québec, Canada J1K 2R1

Received 23 March 2007; received in revised form 31 July 2008; accepted 1 August 2008
Handling Editor: S. Bolton
Available online 30 August 2008

Abstract

Semi-active friction devices are usually designed to dissipate the vibratory energy in a mechanical system by controlling a dry friction interface. When the normal force applied on the friction interface is controlled by a feedback loop, the design of an optimized compensator is challenging due to the complexity of the nonlinear behavior of the dry friction. Usually, with some simplifications, a nonlinear feedback controller can be designed either by the Lyapunov method or by the feedback linearization approach. This paper investigates the interest of narrow-band filtering and phase shift compensation in such nonlinear feedback controllers when the system is excited by an external harmonic force. The complex envelope approach is used to implement the narrow-band filtering with an adjustable phase shift compensation within the nonlinear controllers. Experiments are conducted to validate the control approaches using a friction device composed of two piezoelectric stack actuators, each one applying a normal force on a friction pad in order to stop the movement of a mobile mass excited by a sinusoidal force. The experimental results show that for a proper choice of the phase shift compensation, the sticking period per cycle is reduced, and consequently the power dissipation is increased.

1. Introduction

Due to the limitations of passive measures for reducing noise and vibration at low frequency, smart structures are becoming increasingly important [1]. They offer several advantages in performance over passive techniques because they can be perfectly tuned on the undamped mode or the undesirable vibration. On the other hand, they offer several advantages in implementation over active techniques because they require less energy, less real-time computation and the closed loop system is usually unconditionally stable [2]. The semi-active damping has been implemented with success in many automotive and civil engineering applications especially through viscous friction using electrorheological or magnetorheological fluids [3]. However, semi-active damping devices using energy dissipation through dry friction have been relatively less investigated. These devices assume stable friction phenomena, i.e. without self-excited vibrations [4], and are usually designed to control the dissipation of vibratory energy in a friction device by controlling the normal force

*Corresponding author. Tel.: +1 819 821 8000x62161; fax: +1 819 821 7163.
E-mail address: Philippe.Micheau@USherbrooke.ca (P. Micheau).

0022-460X/$ - see front matter © 2008 Elsevier Ltd. All rights reserved.
doi:10.1016/j.jsv.2008.08.002

applied on the friction contacts [5]. Applications of semi-active dry frictions can be found in large-scale aerospace structures [6], in the damping of flexible manipulators [7], in bolted joint connections [8], in automotive industries for the suspensions [9] or for elastic supports [10].

In this work, an approach is presented where dry friction between two surfaces in relative motion is used to control the vibration in structures by energy dissipation. This could be achieved using a number of devices with controlled friction interfaces bonded to a vibrating structure [11,12]. The normal force can be hydraulically or pneumatically generated [13]. However, piezoelectric actuators are well suited for normal force control because they can both generate large forces and have large bandwidth, allowing to be used for advanced control strategies [14]. The control strategy presented in this paper was developed for an original friction device where the normal force on friction pads is controlled by two piezoelectric stacks [15].

In order to optimize the energy dissipation, the normal force has to be perfectly adjusted at any time by using a controller. However, the design of such feedback controller is challenging due to the complexity of the nonlinear behavior of the dry friction and the uncertainties on the parameters. In fact, friction phenomena are described by a large number of friction models with different parameters [11], and the most advanced models exploit velocity dynamics [14]. The LuGre friction model proposed by Canudas de Wit et al. [16] belongs to the dynamic velocity class of friction models. This model aims at incorporating all friction nonlinearities (pre-sliding displacement, Stribeck effect, frictional memory, viscous friction, varying break away force) using only six parameters. Using this friction model, a nonlinear feedback controller can be designed either by the Lyapunov method or by the feedback linearization approach [10]. When the dynamics of the friction is neglected, these controllers naturally lead to nonlinear static feedback laws. However, in such conditions, the controllers cannot deliver the optimal control of the normal force for maximal energy dissipation. Some authors propose to improve the controller performance by adding an observer of the internal friction dynamics; but this approach requires a perfect identification of the friction parameters [17]. On the other hand, this paper presents an original back box approach which consists to anticipate the sticking in order to avoid the complicated dynamics of the friction phenomena associated to a low velocity. For this purpose, the harmonic excitation problem is considered because the advanced control leads to a positive phase shifted control that can be easily implemented with a phase shift and narrow-band filtering.

The filtering operation is implemented in the feedback loop within the formalism of complex envelopes. This is a signal processing tool widely used in communications to perform narrow-band signal processing [18]. Complex envelopes can be used to implement narrow-band controllers working with harmonic signals [19]. Such an approach was successfully implemented for the active control of pulsed flow [20], for the active control of unstable shear layer [21], for the active damping of a low damped mode [22], and for the decentralized active control of periodic panel vibration [23]. For the semi-active friction devices, this signal processing tool is attractive as it allows to easily assess the effect of narrow-band filtering and phase shift compensation in nonlinear feedback controllers.

The paper is organized as follows; Section 2 presents the modelling of the semi-active friction device while Section 3 is related to the two feedback laws designed either by the Lyapunov method or the feedback linearization approach. The phase shift compensation is then added to the feedback laws and implemented using the complex envelope approach. In Section 4, experimental control results are presented for a clamped-free beam excited by a sinusoidal force.

2. Modelling of the semi-active friction device

2.1. Modelling of the mechanical components

Fig. 1 presents a simplified representation of the semi-active friction device used in this work. A harmonic excitation force, F_{exc}, is applied to a moving mass. A friction pad generates the friction force, $F_f(t)$ at the contact interface. A constant normal force F_N is applied at the interface. The dynamics of the system is modelled by a single degree-of-freedom mass–spring–damper system subjected to the friction force given by

$$F_{\text{exc}} - b\dot{x} - kx - F_f = m\ddot{x}, \tag{1}$$

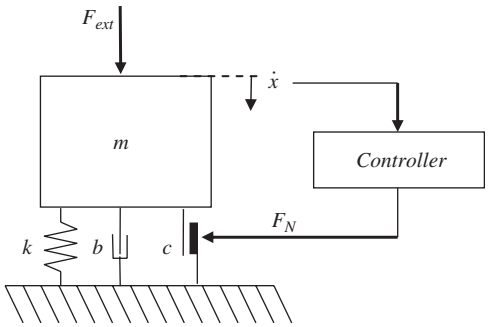

Fig. 1. Mechanical model of the semi-active friction device.

where m is the moving mass, x the relative displacement of the moving mass, k the equivalent stiffness and b the equivalent viscous damping coefficient.

The LuGre model friction model allows a representation of the friction force including rate-dependent effects such sliding bristles (the microscopic contact elements in the model). The representation of the rate-dependent effects is based on an internal friction variable z which can be interpreted as an average deflection of the bristles. The friction force is given as

$$F_f = F_N(\sigma_0 z + \sigma_1 \dot{z} + \sigma_2 \dot{x}), \tag{2}$$

where F_N is the normal force, σ_0 and σ_1 are, respectively, the stiffness and the damping coefficient of the bristles, and σ_2 is the viscous damping coefficient. A relaxation dynamics of the internal variable z is modelled with a nonlinear ordinary differential equation:

$$\dot{z} = \dot{x} - \frac{|\dot{x}|}{g(\dot{x})} z, \tag{3}$$

where the function g is the steady-state friction force as an algebraic function of the relative sliding velocity $\dot{x}$:

$$g(\dot{x}) = \frac{1}{\sigma_0}\left(F_c + (F_s - F_c)\exp\left(-\frac{\dot{x}^2}{v_s^2}\right)\right), \tag{4}$$

where F_c is the Coulomb friction force, F_s is the stiction force, and v_s is the Stribeck velocity. The function $g(\dot{x})$ decreases monotonically from $g(0)$ when $\dot{x}$ increases and this corresponds to the Stribeck effect [16,24].

As long as the system do not exhibit significant rate-dependent effects, it is possible to neglect the bristle dynamics, $\dot{z} = 0$. Consequently, the LuGre friction model is simplified to a static friction law:

$$F_f = F_N c(\dot{x}) \tag{5}$$

with $c(\dot{x}) = \sigma_0 g(\dot{x})\,\mathrm{sgn}(\dot{x}) + \sigma_2 \dot{x}$. The symmetry $-c(\dot{x}) = c(-\dot{x})$ should be noted. The classical Coulomb's friction law with equal static and dynamic friction coefficient is obtained by considering two simplifications: neglected the damping of bristles ($\sigma_2 \approx 0$) and no Stribeck effect ($v_s \approx 0$).

2.2. Modelling of the piezoelectric actuation

During relative motion, a normal force is applied to induce friction force at the contact interface between the moving mass and the friction pads. In the semi-active device, piezoelectric actuators are used to apply the normal force. Each actuator consists of a number of piezoelectric layers in a stack. It is assumed that the electric field is applied only in the thickness direction of the piezoelectric elements [25]. In this case, the linear constitutive equations are:

$$\begin{aligned} \varepsilon_3 &= s_{33}^E \sigma_3 + d_{33} E_3, \\ D_3 &= d_{33}\sigma_3 + \varepsilon_3^{\mathrm{T}} E_3, \end{aligned} \tag{6}$$

where ε_3, σ_3, D_3 and E_3 are, respectively, the strain, stress, electrical displacement (electrical charge per unit area) and the electric field (voltage per unit length). In addition, s_{33}^E, d_{33} and ε_3^T are, respectively, the elastic compliance (the inverse of the elastic modulus), the piezoelectric strain constant and the permittivity of the material.

For practical application, it is convenient to transform Eq. (6) such that physical (measurable) quantities appear. These physical quantities are the displacement w, the force F, the applied voltage U_N and the electrical charge Q [26]. With the area of the actuator A and the thickness of each layer h, the following transformations are then introduced:

$$\varepsilon_3 = \frac{w}{nh}, \quad \sigma_3 = \frac{F}{A}, \quad E_3 = \frac{U_N}{h}, \quad D_3 = \frac{Q}{A}. \tag{7}$$

If F_{ext} is the external force applied on a piezoelectric stack actuator with n thin layers of piezoelectric material, the strain is given by

$$\frac{w}{nh} = s_{33}^E \frac{F_{\text{ext}}}{A} + d_{33} \frac{U_N}{h}. \tag{8}$$

Eq. (8) can be rewritten in the following form:

$$F_{\text{ext}} = k_{\text{pzt}} w - F_{\text{pzt}}, \tag{9}$$

where $k_{\text{pzt}} = A/(nhs_{33}^E)$ and $F_{\text{pzt}} = k_{\text{pzt}} n d_{33} U_N = G_{\text{pzt}} U_N$ are, respectively, the stiffness of the stack actuator and the force generated by the piezoelectric stack actuator with $G_{\text{pzt}} = k_{\text{pzt}} n d_{33}$.

A preload force F_0 is applied to ensure the contact between the surfaces of the moving mass and the frictions pads. The preload results in compression of the equivalent stiffness of the actuator k_{pzt} and of the device itself k_e; the external force measured is then given by

$$F_N = F_0 + \Delta F\, u \tag{10}$$

with $u \in [-1; +1]$. $\Delta F = (k_e/(k_e + k_{\text{pzt}}))G_{\text{pzt}} U_N$ is a modulation term for the preload force F_0 which depends on the piezoelectric stack actuator characteristics, the maximal voltage applied (U_N) and the stiffness of the device itself, k_e. The maximal normal force is given for the command $u = 1$, and the minimal normal force for the command $u = -1$. However, in order to maintain the contact on the friction pads ($F_N > 0$ when $u = -1$), the preload must respect the condition $F_0 > \Delta F$. For the development of the control strategies, the contact between the surfaces is assumed with a null preload force ($F_0 = 0$), and then the command can only be positive: $u \in [0; +1]$. In fact, with an experimental setup, the preload force cannot perfectly ensure contact without the introduction of an undesirable residual constant friction force.

2.3. Trade-off for maximal dissipated energy

The energy dissipated during one cycle corresponds to the work done by the friction force during this cycle and, in the case of harmonic force excitation with period T, is given by the product of the colocated dual variables associated with the mass: the force, F_f, and the velocity, $\dot{x}$:

$$P_d = \frac{1}{T} \oint_{x(t_0)}^{x(t_0+T)} F_f \, \mathrm{d}x = \frac{1}{T} \int_{t_0}^{t_0+T} \dot{x}(t) F_f(t) \, \mathrm{d}t. \tag{11}$$

From Eq. (5), it is possible to control the dissipated power of the device through the normal force applied on the friction pads. But, when the excitation force is harmonic of constant amplitude, the dissipated energy by the friction phenomena reaches an extremal value for an optimal constant normal force on the pads [27]. In order to explain this, let us first consider a constant and a large normal force. This induces a large friction force which opposes a high resistance which in turn reduces the relative displacement amplitude. In the worst case, a too high constant normal force will cancel the energy dissipation by sticking off the surfaces. On the other hand, a small constant normal force induces a small friction force but the relative displacement has a greater amplitude. Again, in the worst case, a too low constant normal force will release the contact which will, in turn, lead to the cancellation of the friction force. So, to obtain maximal dissipated energy with constant normal force control, a trade-off must be achieved between the need to have a large friction force and the need

to have a large relative displacement. In this work, the large bandwidth offered by piezoelectric actuation is exploited to generate a fast time-varying normal force, and then to maximize the energy dissipated.

3. Design of the feedback law

3.1. Nonlinear state space model

In order to allow the design of a feedback law with the Lyapunov method, the system has to be written in the state-space form given as

$$\dot{\mathbf{x}} = \mathbf{f}(\mathbf{x}) + \mathbf{g}(\mathbf{x})u \tag{12}$$

with $\mathbf{x}$ the state vector, u the command signal, and the smooth vector functions $\mathbf{f} : \mathbb{R}^n \to \mathbb{R}^n$ and $\mathbf{g} : \mathbb{R}^n \to \mathbb{R}^n$ defined in $\mathbb{R}^n$.

The friction force expressed by Eq. (5) becomes, with the command of the normal force (Eq. (10)):

$$F_f(\dot{x}, u) = F_0 c(\dot{x}) + \Delta F\, c(\dot{x})u. \tag{13}$$

Hence, the state vector of the system is $\mathbf{x} = [x_1 \;\; x_2]^{\mathrm{T}}$ with $x_1 = x$ and $x_2 = \dot{x}$.

The nonlinear system described by Eq. (12), is now written in terms of the vector functions:

$$\mathbf{f} = \begin{bmatrix} x_2 \\ -\dfrac{k}{m}x_1 - \dfrac{b}{m}x_2 - \dfrac{F_0}{m}c(x_2) \end{bmatrix} \quad \text{and} \quad \mathbf{g} = \begin{bmatrix} 0 \\ -\dfrac{\Delta F}{m}c(x_2) \end{bmatrix}. \tag{14}$$

3.2. Application of the Lyapunov method

A smooth scalar function $V(\mathbf{x}) : \mathbb{R}^n \to \mathbb{R}$ is said to be a Lyapunov function for the system if $V(\mathbf{x}) \geqslant 0$ and has continuous partial derivatives, and $\dot{V} \leqslant 0$. When a Lyapunov function exists, the point $\mathbf{x} = \mathbf{0}$ is stable. In the case presented herein, the total mechanical energy of a system defined as

$$V(\mathbf{x}) = \frac{1}{2}\mathbf{x}^{\mathrm{T}} \begin{bmatrix} k & 0 \\ 0 & m \end{bmatrix} \mathbf{x} \tag{15}$$

is a candidate Lyapunov function.

The time derivative of $V(\mathbf{x})$ along any trajectory of the system is the dissipated power of the system and is given by the following expression:

$$\dot{V}(\mathbf{x}) = L_f V(\mathbf{x}) + L_g V(\mathbf{x})u, \tag{16}$$

where the two new scalar functions, $L_f V(\mathbf{x}) = \nabla V(\mathbf{x})\mathbf{f}(\mathbf{x})$ and $L_g V(\mathbf{x}) = \nabla V(\mathbf{x})\mathbf{g}(\mathbf{x})$, are called the Lie derivatives of $V(\mathbf{x})$ with respect to $\mathbf{f}(\mathbf{x})$ and $\mathbf{g}(\mathbf{x})$ [28]. The gradient defined by a row-vector of elements $(\nabla V(\mathbf{x}))_j = \partial V(\mathbf{x})/\partial x_j$, is equal to $\nabla V(\mathbf{x}) = [k \;\; m]\mathbf{x}$ for this problem. This leads to the following expression:

$$\begin{aligned} L_f V(\mathbf{x}) &= -bx_2^2 - F_0 x_2 c(x_2), \\ L_g V(\mathbf{x}) &= -\Delta F\, x_2 c(x_2). \end{aligned} \tag{17}$$

By considering the symmetry property of $c(x)$, it follows that $L_f V(\mathbf{x}) \leqslant 0$ and $L_g V(\mathbf{x}) \leqslant 0$. Hence, the mechanical system is dissipative, $L_f V(\mathbf{x}) < 0$ and $L_g V(\mathbf{x}) < 0$ when $x_2 \neq 0$ ($\dot{x} \neq 0$). On the other hand, whatever is x_1 (the displacement x), there is no dissipation of mechanical energy ($\dot{V}(\mathbf{x}) = 0$) without velocity ($x_2 = 0$) (Fig. 2).

A special case occurs when the damper sticks. This happens when $x_2 = 0$ and $\dot{x}_2 = 0$ and, in this case, there is no energy dissipation ($\dot{V}(\mathbf{x}) = 0$), and the displacement, $x_1 = F_f(0, u)/k$, can be non-zero because $F_f(0, u)$ is multi-valued, then it is possible for the damper to remain stuck.

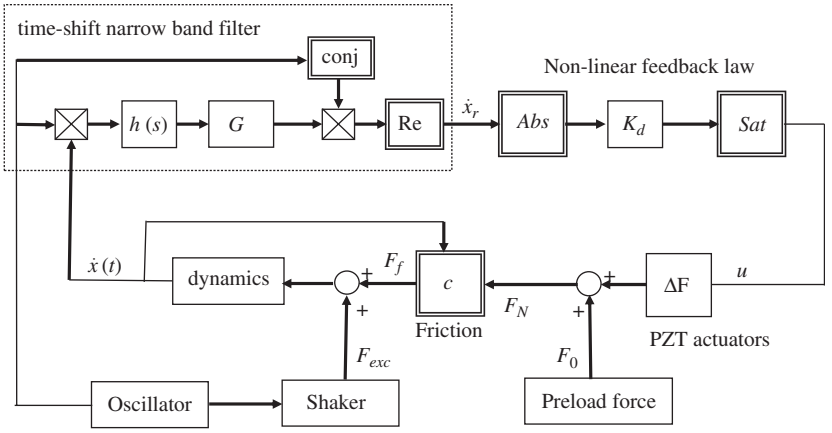

Fig. 2. Scheme of the mechanical system and the nonlinear closed-loop system with phase shift compensation.

3.2.1. Bang–bang controller

In order to maximize energy dissipation, it is necessary to get the maximal value of $-\dot{V}(\mathbf{x})$ associated with a large command $u = U_{\max} \leqslant 1$, but to avoid the special case $\dot{V}(\mathbf{x}) \geqslant 0$ when the damper sticks, associated with a small command $u = U_{\min} \geqslant -1$ (when $\dot{V}(\mathbf{x}) = 0$), or when energy is given to the system (when $\dot{V}(\mathbf{x}) > 0$). Hence, the bang–bang controller applies the maximal force when $\dot{x} \neq 0$, and the minimal one when $\dot{x} = 0$ to prevent the sticking or to release the stuck damper. However, due to noises on the measured velocity and the Stribeck effect, it is preferable to release the normal force when a minimal velocity threshold $\dot{x}_{\min}$ is reached. Hence, the bang–bang controller includes a "*dead zone*" for $\dot{x} \in [-\dot{x}_{\min}; +\dot{x}_{\min}]$:

$$u = \begin{cases} U_{\max} & \text{if } |\dot{x}| > \dot{x}_{\min}, \\ U_{\min} & \text{if } |\dot{x}| \leqslant \dot{x}_{\min}, \end{cases} \tag{18}$$

where $\dot{x}_{\min}$ is a minimal velocity threshold defined by the user. It is important to note that the control law (18) is discontinuous and consequently will generate "*chattering*" (high-frequency switching) in the neighborhood of the switching point ($\dot{x}_{\min}$).

3.2.2. Feedback linearization

The nonlinear system described in Eq. (12) with Eq. (14), is expressed in the controllability canonical form (also called companion form) because $\dot{x}_2 = f_2(\mathbf{x}) + g_2(\mathbf{x})u$ and $\dot{x}_1 = x_2$. For such form, the nonlinearities can be cancelled with a nonlinear feedback law if $g_2(\mathbf{x}) \neq 0$:

$$u = \frac{1}{g_2(\mathbf{x})}(v - f_2(\mathbf{x})), \tag{19}$$

to obtain the simple input–output relation $\dot{x}_2 = v$. Hence, a linear state feedback can be applied $u = -\mathbf{K}x$ with $\mathbf{K} = [K_p \; K_d]$. However, this approach requires a perfect knowledge of the functions $c(x_2)$ and the parameters used in $f_2(\mathbf{x})$ and $g_2(\mathbf{x})$.

A simplified solution can be considered under assumptions. The first one is that $F_0 \approx 0$ (no friction effect when $u = 0$); consequently, $f_2(\mathbf{x}) = [-k/m - b/m]\mathbf{x}$ is linear. The second one is that $\sigma_2 \approx 0$ (the damping of bristles is neglected) and the third one is that $v_s \approx 0$ (no Stribeck effect). Under these assumptions, $g_2(\mathbf{x}) \approx -(\Delta F/m)\sigma_0 F_c \operatorname{sgn}(x_2)$. Hence, the nonlinear feedback law only concerns $g_2(\mathbf{x})$, and is for $u \in [0; +1]$ (because $F_0 \approx 0$):

$$u = K_p b \operatorname{sgn}(\dot{x})x + K_d b|\dot{x}|. \tag{20}$$

In this case, the dynamics of the controlled system is governed by

$$\ddot{x} = -\left(\frac{k}{m} + bK_p\right)x - bK_d\dot{x}. \tag{21}$$

It appears that the feedback gain K_p modifies the resonant frequency and the feedback gain K_d introduces a damping effect. Due to the limited available effort ($u \in [0;1]$) the input saturate for $|\dot{x}| > 1/K_d$. Hence, the practical simplified feedback law is given with $K_p = 0$ (because there is no need to tune the resonant frequency:

$$u = \begin{cases} 1 & \text{if } |\dot{x}| > 1/K_d, \\ K_d|\dot{x}| & \text{if } |\dot{x}| \leqslant 1/K_d. \end{cases} \tag{22}$$

For $K_d \to \infty$, the feedback law, Eq. (22), becomes analogous to the bang–bang controller described by Eq. (18), without the dead-zone, i.e. $\dot{x}_{\min} = 0$.

3.3. Phase compensation for a sinusoidal motion

This section describes a pre-processing approach, implemented as a filter introduced in the feedback loop, in order to correct two major problems associated impairing the performance of nonlinear controllers: unobserved dynamics and sensitivity to noise.

When neglecting the dynamics of the friction, the bang–bang controller and the feedback linearization controller lead to the implementation of a nonlinear static feedback laws: the normal force is a nonlinear function of the mass velocity. However, delays and phase shift in the feedback loop occur in practice and arise from the internal dynamics of the electronic components (sensor pre-amplifiers, PZT amplifiers, anti-aliasing filters, data sampling). These various dynamic behaviors can be isolated and characterized easily. However, the neglected complex dynamics at the dry friction interface is more difficult if not impossible to characterize. As they both rely on a perfect knowledge of the dynamics of the system, the bang–bang and feedback Lyapunov controllers cannot provide the optimal control of the normal force because part of the dynamics was neglected in the design process. However, it may be possible to improve the performance of the nonlinear controllers by adding an observer of the internal friction dynamics and by compensating the effects of the electronic components; but such an approach requires a challenging identification of the six LuGre model parameters [17]. Again, such an approach will perform optimally if and only if the nonlinear model of the friction captures all the dynamics. As an alternative, this paper addresses an original black box approach (not based on any model): a compensator is added in the loop in order to anticipate the sticking of the friction pads. In general terms, the idea is to generate the command to release the normal force before the sticking is observed. Consequently the sticking cannot occur, and there is no need to control the dynamics of the bristles. However, the anticipation of the sticking is a challenging problem with a feedback controller because only the past velocity measurements can be used to generate the present normal force command. However, when the disturbance is periodic with period T, the anticipation is equivalent to perform a positive phase shift control. Hence, in the context of this paper, and for the purpose of the demonstration, the harmonic excitation problem is considered because it leads to a positive (advance) phase shift in the loop at the frequency of the excitation.

The method to avoid the "*chattering*" with the control law given by Eq. (18) consists to filter the velocity signal prior to the generation of the control signal. In order to ensure power dissipation on the friction pads, the velocity must be periodic. A narrow-band filtering centered on the frequency on excitation should dramatically reduce the sensitivity to noise, and consequently limit "*chattering*" to a minimum level. Moreover, such narrow-band filtering can also be applied to the velocity used in the control law given by Eq. (22) in order to avoid added noise on the input signal when a large gain is used.

In order to advance the velocity signal in the feedback loop and to filter the velocity measurement, it is proposed herein to use a narrow-band filter implemented with a complex envelope method [19]. The complex envelope is a complex function of time, and it is the generalization of the phasor concept [18]. Such compensator performs the demodulation of the velocity signal $\dot{x}(t)$ in order to obtain its instantaneous phasor (complex envelope) $\dot{X}(t) \in \mathbb{C}$ of the sinusoid at the frequency ω_0:

$$\dot{X}(t) = \int_0^\infty h(\tau)\dot{x}(t-\tau)\exp(-\mathrm{i}\omega_0(t-\tau))\,\mathrm{d}\tau, \tag{23}$$

where $h(t)$ is a low-pass filter impulse response.

The phase shift operation is applied on this complex signal to generate the instantaneous phasor (complex envelope) of the command $\dot{X}_r(t) \in \mathbb{C}$ by a multiplication:

$$\dot{X}_r(t) = G\dot{X}(t), \tag{24}$$

where $G = \exp(i\Phi)$ is a complex gain and Φ the desired phase shift. Finally, the compensated signal is generated by modulation of the sinusoid at the frequency ω_0:

$$\dot{x}_r(t) = \mathrm{Re}(\dot{X}_r(t)\exp(+i\omega_0 t)), \tag{25}$$

where $\mathrm{Re}(\cdot)$ denotes the real part of $(\cdot)$. By considering the Fourier transform of Eqs. (25), (23), and (24), it can be demonstrated that the proposed compensator is equivalent to a narrow-band compensator centered on the central frequency ω_0:

$$\frac{\dot{x}_r(\omega)}{\dot{x}(\omega)} = -Gh(\omega - \omega_0) - G^* h(-\omega - \omega_0), \tag{26}$$

where G^* is the conjugate of G. With this compensator, the velocity signal is narrow-band filtered. Eq. (25) shows that the proposed controller is a useful and simple way to advance and to filter the measured velocity by setting the phase shift, Φ, at the excitation frequency, ω_0.

4. Experimental validation of the semi-active device

4.1. Presentation of the device

To validate the semi-active device concept, a prototype was designed and fabricated [15]. Fig. 3 shows the semi-active device prototype which has the overall dimensions of 8.5 cm × 5.0 cm × 10.0 cm for a total weight of 1.20 kg. The device includes two flexible phosphorus–bronze alloy blades with 0.41 mm thickness which are attached to the moving mass made of stainless steel. The two flexible blades are clamped to the rigid frame. On each side of the moving mass, friction pads made from car brakes material are assembled. During relative displacement of the mass, normal forces, provided by preload and two piezoelectric stack actuators on both sides of the moving mass, induce friction force at the interface contact between moving mass and frictions pads surfaces. To ensure that this normal force remains perpendicular to the motion of the moving mass and to correct possible misalignment due to the motion (coming, for example, from slight deviated blades), balls are inserted between the friction pads and the piezoelectric actuators. The PZT stack actuators used to apply the normal force are *BM*532 elements from *Sensor Technology Limited* and consist of 78 layers, each layer having

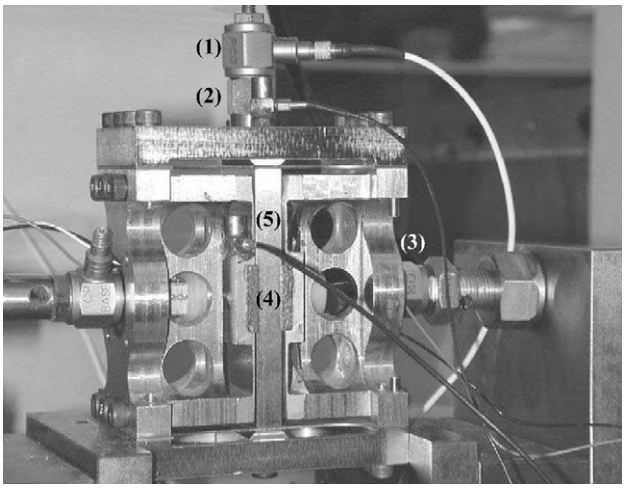

Fig. 3. The semi-active friction device: force sensor (1), accelerometer (2), piezoelectric actuator (3), friction pad (4), and moving mass (5).

0.25 mm thickness. The maximal free displacement is about 9 μm for an applied voltage of 200 V. The maximal force (1200 N) is generated in completely clamped conditions (blocking force).

4.2. Experimental setup

The device presented in Section 4.1 is connected to a beam. An electromagnetic shaker with a power amplifier is used to provide the excitation force at the frequency $f = 60$ Hz with an amplitude of 10 N. This force is measured using a force sensor. The preload is set to $F_0 = 70$ N. The maximal voltage applied to the piezoelectric actuator is $U_N = 200$ V. Two accelerometers are used for the measurement of the relative acceleration between the moving mass and the friction pads.

The signals obtained from the force sensor and accelerometers are conditioned with charge amplifiers and then filtered by an elliptic low-pass filter with a cut-off frequency of 600 Hz (eighth order, 8 poles, and 6 zeros) from *Frequency Devices*, as an anti-aliasing filter. A Butterworth filter (eighth order, 8 poles) is used for filtering shaker and PZT stack actuators control signals.

The controllers are developed within MATLAB/Simulink and implemented on *dSPACE* boards for real time signal processing; visualization and data acquisition are performed under the *ControlDesk* software. The velocity signal is numerically computed, on-line and in real-time in the *dSPACE* system, by numerical high-pass filtering and integration of the measured acceleration. The high-pass filtering is necessary to avoid any drift of the estimated velocity.

4.3. Bang–bang controller

With the bang–bang controller given by Eq. (18), with the compensator given by Eq. (26), the maximal voltage $U_{\max}$ is adjusted from 0 V to +160 V with steps of 5 V. The dead zone is adjusted with $\dot{x}_{\min} = 0.002$ m/s. Fig. 4 presents the dissipated power versus the control parameters: the maximal command, $U_{\max}$ is normalized and is adjusted from 0 to 0.8 with steps of 0.025, the phase shift, Φ is adjusted between 0 and 2π rad. Without the phase shift compensation ($\Phi = 0$ rad), the dissipated power increases from 30 to 100 mW when $U_{\max}$ varies from 0 to 0.4; after the value of 0.4, corresponding to $U_{\max} = 80$ V, the dissipated power dramatically decreases. When the phase shift in the feedback loop varies, the dissipated power is

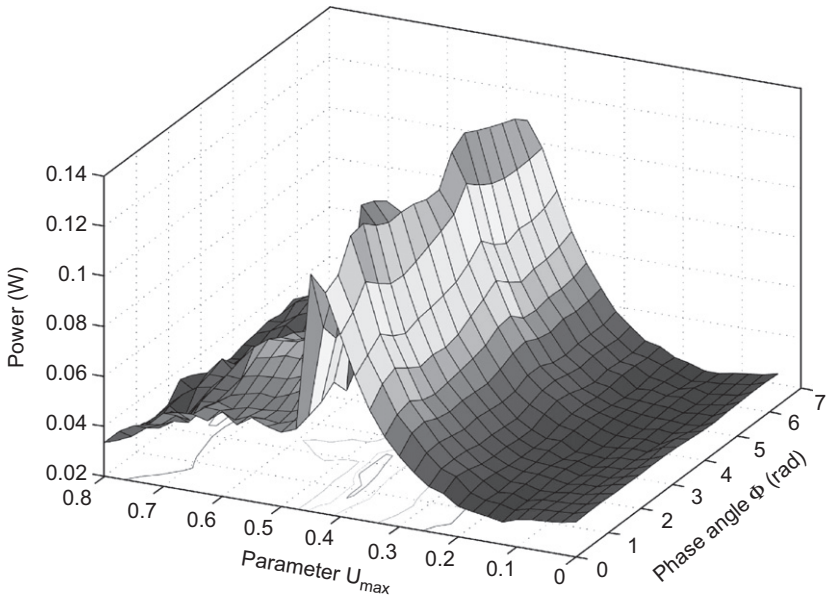

Fig. 4. Power dissipated as a function of the phase angle Φ and actuator control parameter $U_{\max}$ with the bang–bang controller.

modulated with a periodicity of π. The maximal dissipated power of 130 mW is obtained at $U_{\max} = 0.40$ and $\Phi = 1.2$ rad. Hence, a positive phase shifted control allows to optimize the dissipated power by 30%. This results clearly shows, that to obtain a large dissipated power, it is necessary to make a compromise between a large normal force which leads to a small displacement or a small normal force which leads to a large displacement. This result is consistent with similar results obtained by controlling a constant normal force [27].

4.4. Feedback linearization

4.4.1. Optimal tuning

For the case of the feedback linearization controller given by Eq. (22), with the compensator given by Eq. (26), Fig. 5 presents the dissipated power versus the control parameters: the derivative gain K_d and the phase shift Φ. Without control, $K_d = 0$, the dissipated power is 60 mW.

Without the phase shift compensation ($\Phi = 0$ rad), the dissipated power increases from 60 to 102.5 mW when the derivative gain K_d varies from 0 to 32; after, it decreases when the derivative gain K_d is superior than 32. Hence, it is preferable to adjust the derivative gain K_d at 32, or slightly less than 32, but not larger than this value.

When the phase shift in the feedback loop varies between 0 and 2π rad, the dissipated power is modulated with a periodicity of π because the control force is a function of the velocity modulus. In the best case, when the derivative gain K_d is close to 32, the dissipated power varies between 102.5 mW (without phase shift) and 132.5 mW (with an optimal phase shift of $\Phi = 1.2$ rad or $\Phi = 1.2 + \pi$ rad). Finally, the maximal dissipated power of 132.5 mW is obtained for the optimal values of $K_d = 32$ and $\Phi = 1.2$ rad.

4.4.2. Instability of the feedback loop

Without phase shift compensation, i.e. for $\Phi = 0$ rad, the closed-loop becomes unstable for $K_d \geqslant 36$: a self-oscillation occurs at 5 Hz. Fig. 6 presents the instability of the actuator command for $K_d = 36$. The reason for this instability is the narrow-band filtering obtained by the fourth order low-pass filtering filter with a cut-off frequency at 6 Hz since it introduces a -180° phase shift at 6 Hz. With the phase shift it is possible to stabilize this feedback loop with the value $\Phi = \pi/2$ rad when $K_d > 36$. However, the compensator was not introduce in

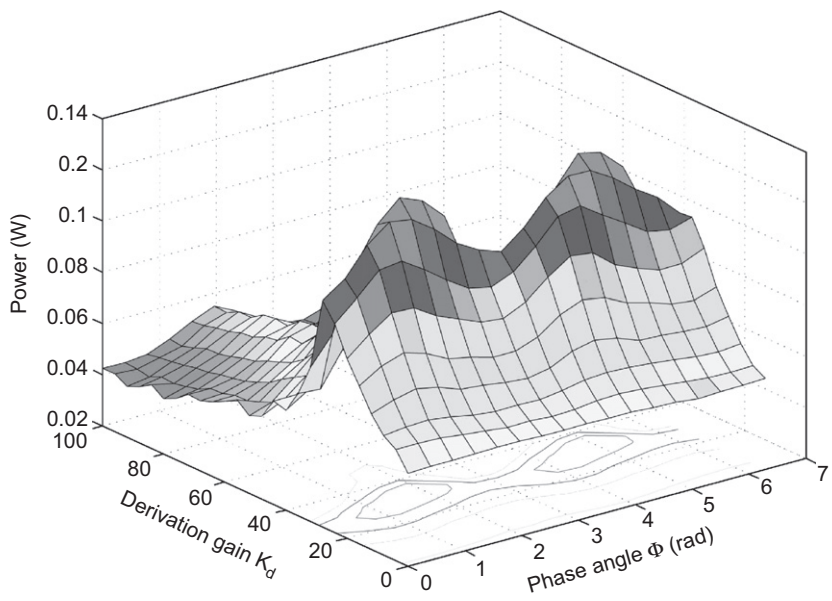

Fig. 5. Power dissipated as a function of the derivative gain K_d and phase angle Φ.

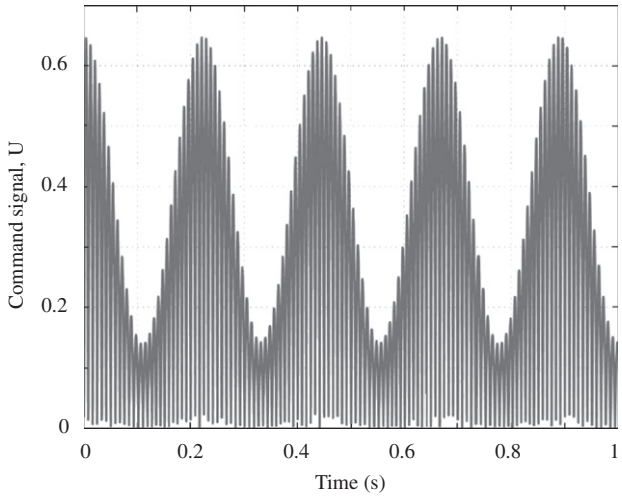

Fig. 6. Instability for $K_d = 36$ and $\Phi = 0$ rad due to the narrow-band filtering at 6 Hz.

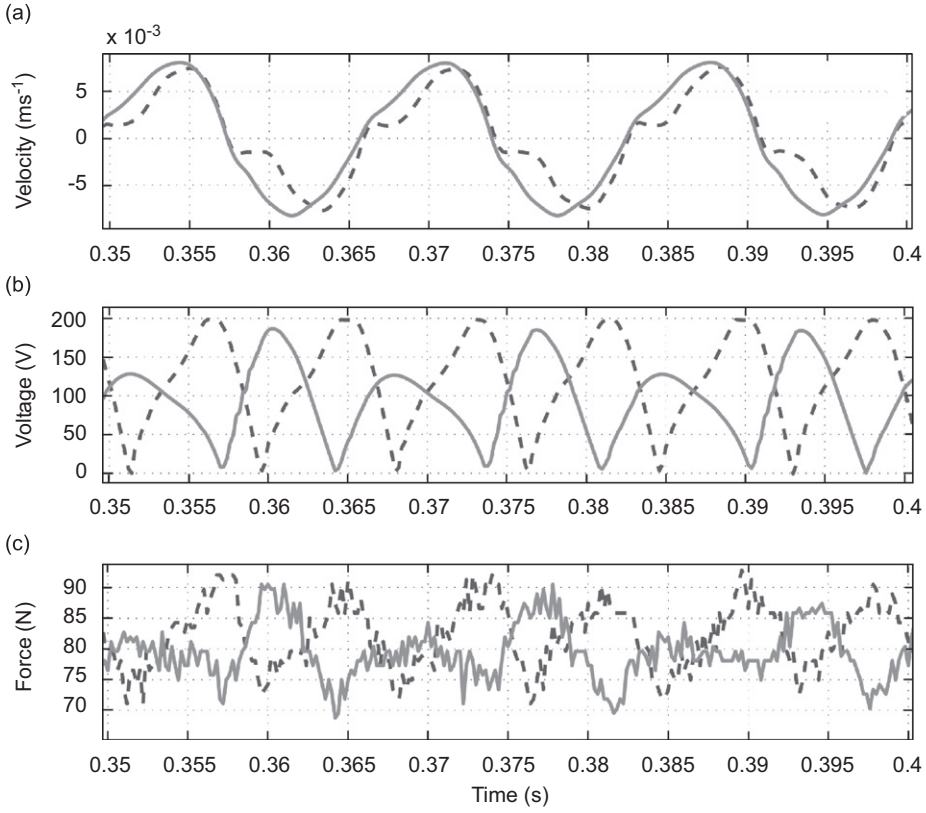

Fig. 7. Velocity (a), actuator voltage (b), and normal force (c) for $K_d = 200$, without phase shift $\Phi = 0$ rad (dot line) and with phase shift $\Phi = 0.5$ rad (plain line).

the loop to stabilize it. Hence, in order to increase the gain margin, without the tuning of a phase shift, the low-pass filter is replaced by a second order elliptic filter with an higher cut-off frequency at 95 Hz. Experimental results validated that a large value of the derivative gain can now be used without risk of instability.

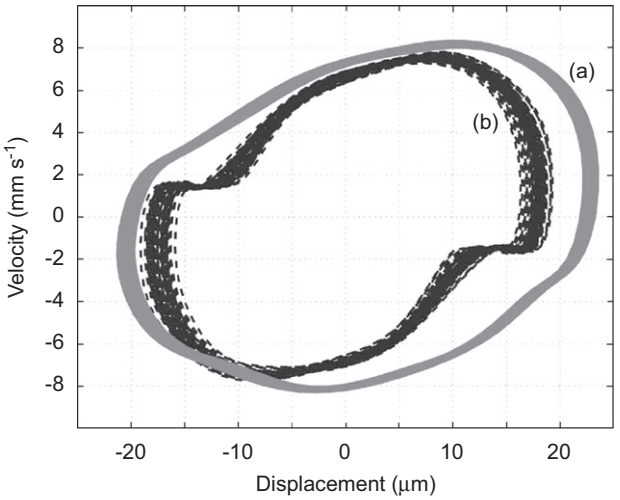

Fig. 8. Phase diagram for $K_d = 200$, without phase shift $\Phi = 0$ rad (b) and with phase shift $\Phi = 0.5$ rad (a).

4.4.3. Analysis of the system

With the second order elliptic filter introduced in the previous section, Fig. 7 presents a typical result obtained with a derivative gain K_d of 200. The velocity, the voltage on the actuators, and the normal control force are presented for the cases without phase shift compensation, $\Phi = 0$ rad, and with an optimal phase shift compensation of $\Phi = 0.5$ rad. Due to the preload of 70 N, the normal force is modulated between 70 and 90 N by the actuator voltage. It clearly appears that the measured normal force is perfectly in-phase with the voltage control applied to the PZT stack.

For the case $\Phi = 0$ rad, the velocity shows a significant sticking time per cycle: the velocity is close to zero from $t = 0.357$ to 0.360 s, for example. The end of sticking is due to the release of the normal force: at time $t = 0.360$ s, the normal force is close 72 N, for example. On the other hand, for the case $\Phi = 0.5$ rad, there is no sticking time per cycle. The impact of the phase shift compensation on the dissipated power is clearly visible in Fig. 8 which presents the velocity versus the displacement, because the area of drawn by such curves is the dissipated power. Without phase shift compensation, for $\Phi = 0$ rad, the sticking limits the dissipated power. The sticking disappears when a $\Phi = 0.5$ rad phase shift compensation is applied; the dissipated power is then increased by 25%.

5. Conclusions

We have presented an original nonlinear feedback loop to control a device designed to dissipate the vibratory energy by controlling a dry friction force. Experimental setup was an original device composed of friction pads acting on a mobile component; the normal force on the pads are under control of piezoelectric stack actuators characterized by a large bandwidth. The results have shown that it exists an optimal tuning of the feedback loop parameters which are the amplitude and the phase shift for the bang–bang controller, and the derivative gain and the phase shift for the feedback linearization controller. In both cases, it exists a proper choice of the phase shift compensation that can improve the power dissipation. It is however worth noticing that the two nonlinear control strategies presented are based on a simplified model of the friction phenomena; but the phase shifted normal force allows to anticipate the sticking and consequently allows to optimize the friction dissipation. Consequently, the proposed nonlinear feedback laws with phase shift control are good candidates to improve the control of friction dampers.

Acknowledgments

This work was supported by the National Science and Engineering Research Council (NSERC) and by the Network of Centres of Excellence AUTO21, Canada.

References

[1] S. Hurlebaus, L. Gaul, Smart structure dynamics, *Mechanical Systems and Signal Processing* 20 (2) (2006) 255–281.
[2] C. Fuller, S. Elliot, P. Nelson, *Active Control of Vibration*, Academic Press, London, 1996.
[3] N. McClamroch, H. Gavin, Electrorheological dampers and semi-active structural control, *Proceedings of 34th Conference on Decision and Control*, New-Orleans, LA, 1994, pp. 3528–3533.
[4] N. Hoffmann, Linear stability of steady sliding point contacts with velocity dependent and Lugre type friction, *Journal of Sound and Vibration* 301 (2007) 1023–1034.
[5] D. Karnopp, M. Crosby, R. Harwood, Vibration control using semi-active force generators, *Journal of Engineering for Industry* 96 (2) (1974) 619–626.
[6] J. Lane, Control of Dynamic Systems Using Semi-active Friction Damping, PhD Thesis, Georgia Institute of Technology, 1992.
[7] J. Lane, S. Dickerson, Contribution of passive damping to the control of flexible manipulators, *Proceedings of ASME Computers in Engineering*, Las Vegas, NV, 1984, pp. 175–180.
[8] L. Gaul, R. Nitsche, Friction control for vibration suppression, *Mechanical Systems and Signal Processing* 14 (2) (2000) 139–150.
[9] A. Ferri, B. Heck, Semi-active suspension using dry friction energy dissipation, *Proceedings of the 1992 American Control Conference*, Chicago, IL, 1992, pp. 31–35.
[10] M. Lorenz, B. Heimann, J. Tschimmel, V. Hartel, Applying semi-active friction damping to elastic supports for automotive applications, *Proceedings of IEEE ASME International Conference on Advanced Intelligent Mechatronics*, Kobe, Japan, 2003.
[11] B. Armstrong-Hélouvry, P. Dupont, C. Canudas de Wit, A survey of models, analysis tools and compensation methods for the control of machines with friction, *Automatica* 30 (7) (1994) 1083–1138.
[12] O. Durmaz, W.C. Clark, D. Bennett, S. Paine, Jeffrey, M. Samuelson, Experimental and analytical studies of a novel semi-active piezoelectric coulomb damper, *Proceedings of SPIE Smart Structures and Materials 2002*: *Damping and Isolation*, San Diego, CA, 2002, pp. 258–273.
[13] C.W. Stammers, T. Sireteanu, Vibration control of machines by using of semi-active dry friction damping, *Journal of Sound and Vibration* 209 (4) (1997) 671–684.
[14] P. Dupont, P. Kasturi, A. Stokes, Semi-active control of friction dampers, *Journal of Sound and Vibration* 202 (2) (1997) 203–218.
[15] P. Buaka, Development of a Semi-active Device for Attenuation of Vibrations in Mechanical Structures by Energy Dissipation with Dry Friction, PhD Thesis, Université de Sherbrooke, 2005 (in French).
[16] C. Canudas de Wit, H. Olsson, K. Astrom, A new model for control of systems with friction, *IEEE Transactions on Automatic Control* 40 (3) (1995) 419–425.
[17] L. Gaul, R. Nitsche, Lyapunov design of damping controllers, *Journal of Applied Mechanics* 72 (2003) 865–874.
[18] L. Couch, *Digital and Analog Communications Systems*, sixth ed., Prentice-Hall, Upper Saddle River, NJ, 2001.
[19] P. Micheau, P. Coirault, Adaptive controller using filter banks to reject multi-sinusoidal disturbance, *Automatica* 36 (2000) 1659–1664.
[20] P. Micheau, P. Coirault, L. Hardouin, J. Tartarin, Adaptive rejection of the preponderant harmonic of a pulsed flow, *IEEE Transactions on Control System Technology* 4 (1996) 452–458.
[21] P. Micheau, L. Chatellier, J. Laumonier, Y. Gervais, Stability analysis of active control of self-sustained pressure fluctuations due to flow over a cavity, *Journal of the Acoustical Society of America* 119 (3) (2006) 1951.
[22] S. Renault, P. Micheau, Active control of the complex envelope associated with a low damped mode, *Mechanical and Signal Processing* 20 (3) (2006) 646–661.
[23] M. Baudry, P. Micheau, A. Berry, Decentralized active vibration control of a flexible plate using piezoelectric actuator—sensor pairs, *Journal of the Acoustic Society of America* 119 (1) (2006) 262–277.
[24] R. Hensen, Controlled Mechanical Systems with Friction, PhD Thesis, Technische Universiteit Eindhoven, 2002.
[25] W. Heverly, E. Smith, Dual-stack piezoelectric device with bidirectional actuation and improved performance, *Journal of Intelligent Material Systems and Structures* 15 (2004) 565–574.
[26] E. Colla, T. Monita, Piezoelectric technology for active vibration control, *Piezoelectric Materials in Devices* (2002) 123–154.
[27] P. Buaka, P. Masson, P. Micheau, Determination of normal force for optimal energy dissipation of harmonic disturbance in a semi-active device, *Journal of Sound and Vibration* 311 (2008) 633–651.
[28] J. Slotine, W. Li, *Applied Nonlinear Control*, Prentice-Hall, Englewood Cliffs, NJ, 1991.